Available online at www.sciencedirect.com
SCIENCE DIRECT
Journal of Photochemistry and Photobiology A: Chemistry xxx (2005) xxx–xxx
Journal of Photochemistry and Photobiology A:Chemistry
www.elsevier.com/locate/jphotochem

Photolysis of sulfosalicylic acid in aqueous solutions over a wide pH range

Ivan P. Pozdnyakov [a,*], Victor F. Plyusnin [a], Vjacheslav P. Grivin [a], Dmitry Yu. Vorobyev [a], Nikolai M. Bazhin [a], Eric Vauthey [b]

[a] *Institute of Chemical Kinetics and Combustion, Institutskaya 3, 630090 Novosibirsk, Russia*
[b] *Department of Physical Chemistry, University of Geneva, 30 quai Ernest Ansermet, 1211 Geneva, Switzerland*

Received 3 June 2005; received in revised form 29 September 2005; accepted 24 October 2005

Abstract

Nanosecond laser flash photolysis, absorption and fluorescent spectroscopy were used to study the influence of pH on the photophysical and photochemical processes of 5-sulfosalicylic acid (SSA) in aqueous solutions. Information on the excited singlet state intramolecular proton transfer (ESIPT) of the SSA ions could be deduced from the dependence of the quantum yield and the spectral maximum of SSA fluorescence on the pH of the medium. The main photochemical active form of SSA at pH < 10 is the dianion ($HSSA^{2-}$). Excitation of this species gives rise to the $HSSA^{2-}$ triplet state, to the $SSA^{\bullet 2-}$ radical anion and to the hydrated electron. In a neutral medium, the main decay channels of these intermediates are T–T annihilation, recombination and capture by the $HSSA^{2-}$ dianion, respectively. A decrease of pH leads to an increase of the second-order rate constants of disappearance of both $HSSA^{2-}$ triplet state and $SSA^{\bullet 2-}$ radical anion due to their protonation.

Keywords: Sulfosalicylic acid; Laser flash photolysis; Photoionization; Triplet–triplet absorption; Hydrated electron

1. Introduction

Organic acids ($R–CO_2H$) are a class of compounds abundant in natural water [1]. These acids can form complexes with many transient metals (including Fe(III)) whose photochemistry can contribute substantially to the balance of organic compounds in water [2–9]. It is worth noting that aromatic acids have their own strong absorption bands in the UV range and can be subjected to photochemical transformation under solar radiation in a free noncoordinated state.

Salicylic acid (2-hydroxybenzoic acid) (SA) and its derivatives (SAD) are considered as representatives of the complexing functional groups in humic substances [10] and can serve as model compounds for investigating the photochemical properties of natural acids. In the ground state SA and SAD present by two rotamers A and B (Fig. 1A) [11–13]. Rotamer A is more thermodynamically stable than B (enthalpy difference is 14 and 10 kJ/mol in case of SA and methyl salicylate (MS) [14,15]) due to an intramolecular hydrogen bond. Excitation of rotamer A in the gas phase and in non-polar solvents gives rise to an ultrafast (~60 fs in case of MS [13]) excited state intramolecular proton transfer (ESIPT) from the hydroxyl to the carboxyl group resulting to the formation of a tautomeric form of the acid (Fig. 1B). This accounts for the large stokes shift of SA fluorescence and its derivatives ($\lambda_{em} \approx 440$ nm [11–13,16]). Rotamer B cannot undergo ESIPT and has fluorescence band with maximum at 330 nm.

In protic polar solvents, such as water and ethanol, the fluorescence band maximum of SA and SAD moves to shorter wavelength (400 nm). This is accompanied by an increase of lifetime (from 1 to 6–8 ns) and fluorescence quantum yield [16–19]. This is due to proton transfer to the solvent in the ground state, which results in the formation of the anion of the corresponding acid whose photophysical properties differ from those of the neutral. It is also assumed that in protic polar solvents, the excited state of the neutral and anion forms of SA have zwitterionic and anionic character, respectively (Fig. 1B). In polar solvents, the formation of the proton-transferred instead of the tautomeric form of SA upon excitation is energetically favored

* Corresponding author at: ul. Institutskaja 3, ICK and C SB RAS, 630090 Novosibirsk, Russia. Tel.: +7 3832 332385; fax: +7 3832 307350.
E-mail address: pozdnyak@ns.kinetics.nsc.ru (I.P. Pozdnyakov).

1010-6030/$ – see front matter © 2005 Published by Elsevier B.V.
doi:10.1016/j.jphotochem.2005.10.030

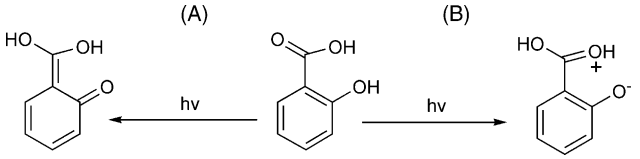

Fig. 1. Primary photoprocesses of the neutral form of salicylic acid in non-polar (A) and polar (B) solvents.

by solvation. According to theoretical calculations on the SA anion, the activation energy for the intramolecular proton transfer from the hydroxyl to the carboxyl group, which can account for the increase of the fluorescence quantum yield of SA in polar solvents [16], amounts to 4 kJ/mol only [14].

In [20], we have studied the photochemistry of 5-sulfocalicylic acid (SSA) in neutral aqueous solutions. In these conditions, the main form of SSA was the $HSSA^{2-}$ dianion. SSA was chosen because of its better solubility in water compared to SA. Excitation of $HSSA^{2-}$ (308 nm, XeCl laser) gives rise to the triplet state of the dianion, to the hydrated electron and to the $HSSA^{\bullet -}$ radical anion. The last two species result from two-photon processes.

In the present work, we report on our investigation of the photophysical and photochemical properties of SSA over a wider pH range (0–10). We expanded the pH range because in natural water, the concentration of the various forms of organic acids and their photoprocesses depend on both their initial concentrations and the pH of the medium.

2. Experimental

A laser flash photolysis set-up (ELI-94 excimer laser operated at 308 nm with pulse duration of 15 ns and mean pulse energy of 20 mJ) was used. The probe light source was a xenon arc lamp DKSSh-150. An increase of the light intensity by a factor of about 100 was achieved by an additional current pulse (∼150 A, ∼1 ms). A fraction of probe light was sent to a photodiode with a quartz plate and was used as feedback signal to stabilize the light intensity.

The excitation and probe light beams were directed to the sample with a small angle (≈2°) through a diaphragm (2 × 7 mm). After the sample, the probe light passed through a monochromator (MDR 23) equipped with a photomultiplier (FEU-84). The transient absorption signal was amplified (up to 256 times) and then directed to a 8 bit-ADC with 1024 counts and a time resolution of 50 ns. With this PC-controlled set-up, absorption changes as small as 5×10^{-4} could be measured.

The fluorescence spectra were measured on a Varian CARY Eclipse spectrofluorimeter (λ_{ex} = 300 nm). The absorption spectra were recorded using an HP 8453 spectrophotometer. The NMR spectra were obtained with a DPX-200 Bruker spectrometer (200 MHz). Chromatographic analysis was performed using a HPLC SP8800-20 "Spectra-Physics" chromatograph (column 4 × 150 mm, Lichrospher RP-18, 5 μm; UV-detector: recording wavelength 220 nm; solvents: A-water, B-acetonitrile; gradient-linear: 0 min-0% B, 20 min-85% B; flow rate: 1.0 ml/min, injection 50 μl).

The fluorescence quantum yield of SSA was determined as described in [21] using solutions of anthracene in ethanol ($\phi = 0.27$) and quinine bisulfate in 1 M H_2SO_4 ($\phi = 0.546$) as standards. The laser pulse power was estimated using solutions of anthracene in benzene. The extinction coefficient of anthracene T–T absorption (TTA) in this solvent at 431 nm amounts to $\varepsilon = 4.2 \times 10^4\ M^{-1}\ cm^{-1}$ and the triplet yield is $\phi_T = 0.53$ [22].

SSA (99+%, Aldrich) was employed without further purification. The solutions were prepared using bidistilled water. Unless otherwise specified, all experiments were carried out with oxygen-free samples in a 1 cm optical cell at 298 K. Oxygen was removed by bubbling solutions with gaseous nitrogen.

3. Results and discussion

3.1. SSA photophysics

The absorption spectra of SAD are determined by the π-system of the aromatic ring interacting with the additional π-bond on the C=O group of the acid residue. Indeed, if the absorption band of phenol in aqueous solutions is centered at 270 nm ($\varepsilon = 1.5 \times 10^3\ M^{-1}\ cm^{-1}$), SA has a fairly strong absorption band at 300 nm (λ_{max} = 303 nm, $\varepsilon = 3.5 \times 10^3\ M^{-1}\ cm^{-1}$) [23]. The absorption band of SA shifts to the red upon substitution [16].

SSA has three acid protons (H_3SSA) that can dissociate in aqueous solutions. The SO_3H proton has a $pK_a < 0$, while the COOH and OH protons have a pK_a of 2.9 and 11.8, respectively [24]. Absorption spectrum of SSA (Fig. 2) does not exhibit substantial changes over the pH range of 0–10 due to the similar spectral properties of H_2SSA^- and $HSSA^{2-}$ ions (Table 1). At pH > 12, the absorption spectrum exhibits a new band with a maximum at 260 nm ($\varepsilon = 1.56 \times 10^4\ M^{-1}\ cm^{-1}$), which corresponds to acid tri-anion (SSA^{3-}). In non-polar solvents at high concentration of SAD formation of dimeric species is observed [11,25]. In aqueous solutions of SSA no evidence for formation dimeric species was found in the range 10^{-5}–10^{-2} M of SSA.

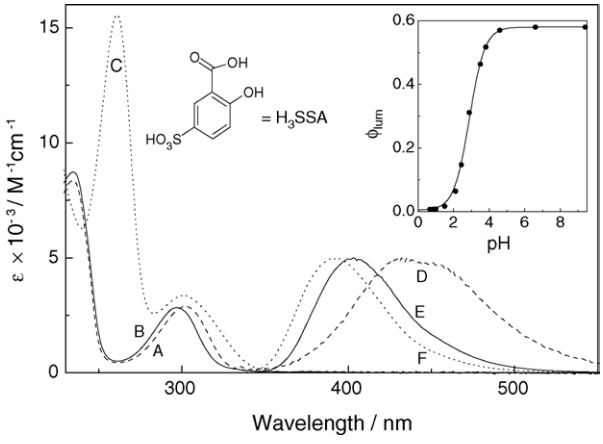

Fig. 2. Absorption (A, B, C) and fluorescence (D, E, F) spectra of SSA ions in aqueous solutions: (A, D) monoanion H_2SSA^- ($HClO_4$, pH = 0.7); (B, E) dianion $HSSA^{2-}$ (NaOH, pH = 7.2); (C, F) tri-anion SSA^{3-} (NaOH, pH = 13). Inset: pH dependence of the quantum yield of SSA fluorescence.

Table 1
Absorption and fluorescent properties of SSA ions

Species	λ_{max}^{abs} (nm)	ε_{max} ($\times 10^{-3}$ M^{-1} cm^{-1})	λ_{max}^{lum} (nm)	φ_{lum}[a]
H_2SSA^-	302	2.8	440	0.011
$HSSA^{2-}$	297	2.8	404	0.58
SSA^{3-}	302	3.3	391	0.26

[a] Standard error ± 20%.

All three forms of SSA exhibit large stokes shift of fluorescence (Fig. 2, Table 1) indicating on ESIPT. The fluorescence maximum shifts to shorter wavelength upon transition from the mono-(H_2SSA^-) to the di-($HSSA^{2-}$) and further to the tri-anion (SSA^{3-}) forms of the acid (Fig. 2, Table 1). In the case of SA, the fluorescence maximum moves from 440 to 405 nm [17,19] when going from the neutral (H_2SA) to the monoanion form (HSA^-). Thus, the addition of a SO_3H group to the SA does not affect the position of the fluorescence maximum. It worth noting, that excitation spectra of individual SSA forms coincide very well with absorption one. The pH dependence of the fluorescence quantum yield (φ_{fl}) of SSA exhibits a S-shape with the inflection point at pH = 2.9 (Fig. 2, insert). This value coincides with the dissociation constant of the SSA COOH group ($pK_a = 2.9$). Thus, the increase in φ_{fl} with increasing pH is due to the deprotonation of the carboxylic group of the acid.

Quantum yield of H_2SSA^- luminescence is more than one-order lower comparing to the $HSSA^{2-}$ and SSA^{3-} forms (Table 1). This fact could be explained by formation of unstable zwitterion in excited singlet state of H_2SSA^- due to proton transfer from hydroxyl to carboxyl group of the ion. Similar hypothesis was proposed in [19] to explain one-order decrease of luminescence life-time upon transition from the monoanionic to the neutral form of SA in aqueous solution. From the other hand, large Stokes shift of fluorescence was observed even for tri-anion SSA (Table 1) which has completely deprotonated carboxyl and hydroxyl groups. This fact allows one to conclude that SSA in S_1 state undergoes distortion of entire molecular skeleton due to tautomerization rather than "localized" proton transfer. The former process is assumed to take place in excitation of SA derivatives in gas phase and non-polar solvents [11–13]. From our steady-state data it is impossible to decide clearly which process takes place in excited state of SSA. One needs to use time-resolved fluorescence technique for better understanding of photophysics of SSA in aqueous solutions.

The photochemistry of the mono- and dianion of SSA is considered further, because these species are dominant in aqueous solutions over the pH range typical for natural water.

3.2. SSA photochemistry

In [20], it was shown that excitation of the $HSSA^{2-}$ dianion (XeCl laser, 308 nm) gives rise to the triplet state ($\lambda_{max} = 470$ nm, $\varepsilon_{470} = 6.7 \times 10^3$ M^{-1} cm^{-1}), to the hydrated electron ($\lambda_{max} = 720$ nm, $\varepsilon_{720} = 1.84 \times 10^4$ M^{-1} cm^{-1} [26]) and to the $HSSA^{\bullet -}$ radical anion. The latter two are formed by absorption of a second photon by the singlet state of $HSSA^{2-}$ [20].

$$S_0—h\nu \rightarrow S_1—\text{ESIPT} \rightarrow S_1'—h\nu \rightarrow e_{aq}^- + HSSA^{\bullet -} \quad (1)$$

In addition to photoionization, which is only important under high laser intensity (>40 mJ/cm^2), the main decay channels of the $HSSA^{2-}$ S_1' state are the intersystem crossing to the triplet (T_1') state ($k_{ISC} = (5.4 \pm 0.9) \times 10^7$ s^{-1}) and the radiative ($k_{ir} = (9.3 \pm 1.8) \times 10^7$ s^{-1}) and nonradiative ($k_{nr} = (1.3 \pm 0.3) \times 10^7$ s^{-1}) deactivations. The rate constants of these various processes have been determined from the life-time of the S_1' state of $HSSA^{2-}$ ($\tau_{fl} = 6.3$ ns [20]) and the quantum yields of fluorescence ($\varphi_{lum} = 0.58$, Table 1) and intersystem crossing ($\varphi_T = 0.34$). The φ_T value was calculated from the initial part of the plot of the triplet yield versus the laser pulse intensity. It should be noted that the triplet quantum yield of the $HSSA^{2-}$ dianion in aqueous solutions exceeds by order of magnitude the triplet quantum yield of the neutral form of SA in organic solvents [12]. This is probably due to an enhancement of nonradiative relaxation in the tautomeric acid form.

3.2.1. Spectrum and decay kinetics of the T_1' state of $HSSA^{2-}$

In oxygen-free neutral solutions, the maximum of the $HSSA^{2-}$ T–T absorption spectrum is at 470 nm (Fig. 3). The observed decay rate constant (k_{obs}^{470}) of the $HSSA^{2-}$ T_1' state depends linearly on the magnitude of the triplet absorbance at 470 nm (Fig. 4), thus allowing the determination of the rate constant of T–T annihilation ($2k_{T-T} = (5.5 \pm 0.5) \times 10^8$ M^{-1} s^{-1}).

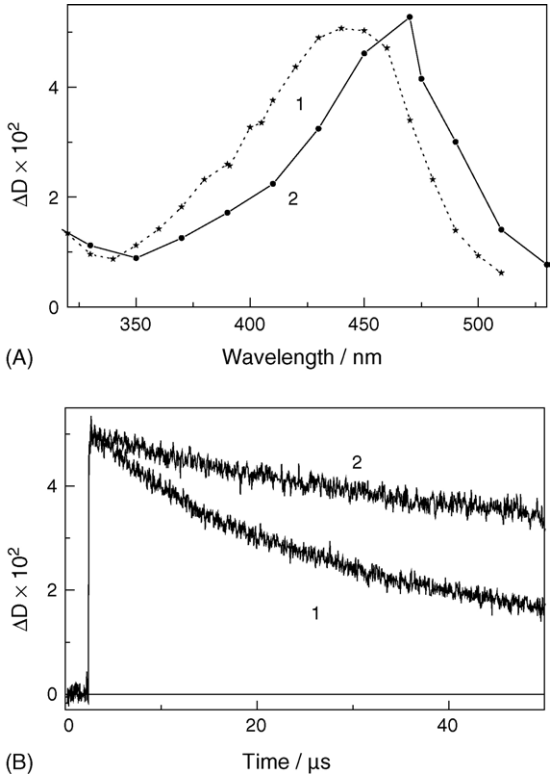

Fig. 3. T–T absorption spectra of: (A) SSA dianion at pH = 3 (1) and 10 (2) recorded just after laser pulse excitation; (B) characteristic kinetic curves at 440 (1) and 470 (2) nm for pH = 3 and 10, respectively. [SSA] = 3.1×10^{-4} M.

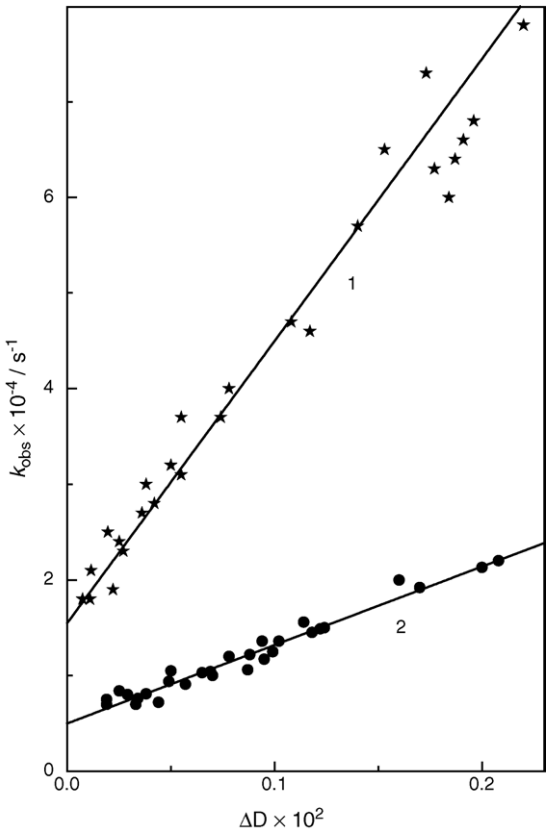

Fig. 4. Dependence of the decay rate constant of the T–T absorption signal, k_{obs}, (1) at 440 nm (pH = 3) and (2) at 470 nm (pH = 10) on the initial optical density. [SSA] = 3.1×10^{-4} M.

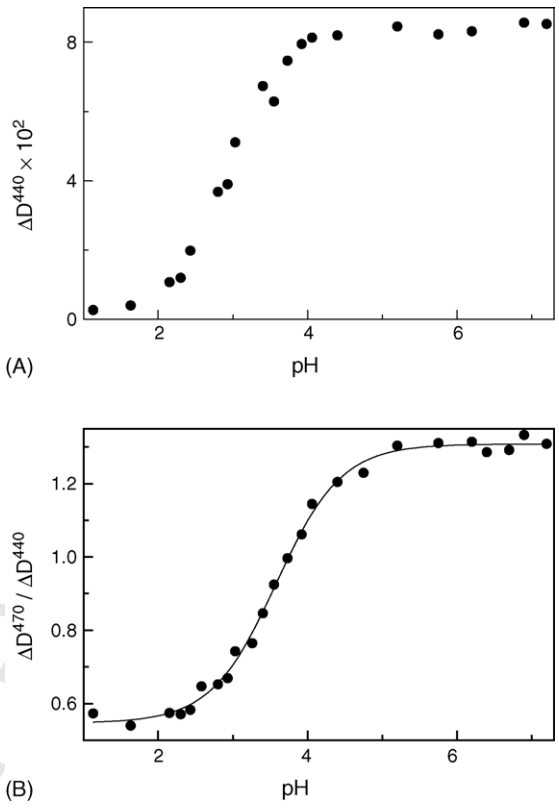

Fig. 5. pH dependence of: (A) ΔD^{440}; (B) the $\Delta D^{470}/\Delta D^{440}$ ratio. The solid line in (B) is the best fit of Eq. (3) with $\varepsilon_1^{440} = 6.2 \times 10^3$ M^{-1} cm^{-1} and pK_2 = 3.5 ([SSA] = 2.6×10^{-4} M).

The small non-zero value of the intercept of the plot in Fig. 4 ($k_{int} \approx 5 \times 10^3$ s^{-1}) corresponds to triplet quenching by residual oxygen (ca. [O_2] $\approx 10^{-6}$ M). Decreasing the pH of the solution causes a shift of the TTA maximum from 470 to 440 nm (Fig. 3) and an increase of k_{obs}^{470} (Fig. 4).

The COOH group of SSA has a pK_a of 2.9 [24]. Therefore, as the pH decreases, a fraction of the light is absorbed by the SSA monoanion (H_2SSA^-). As this species makes almost no contribution to TTA of the sample, the decrease of the pH below four results in a sharp fall-off (Fig. 5A) of the TTA amplitude at 440 nm (ΔD^{440}). The low yield of TTA of the SSA monoanion is explained by a fast radiationless relaxation of the excited singlet state of this species. This is supported by the low fluorescence quantum yield of H_2SSA^- (Table 1). The fast excited state relaxation of SSA monoanion makes a two-photon ionization of H_2SSA^- by a nanosecond laser pulse hardly probable. Thus, the presence of H_2SSA^- in the sample leads only to a decrease in the amount of light absorbed by $HSSA^{2-}$.

The most probable reason for both the shift in the TTA band maximum and the acceleration of the decay kinetics with decreasing pH is the fast (<50 ns) protonation of the hydroxyl group of the SSA dianion in the T_1' state:

$$^TH_2SSA^- \Leftrightarrow {}^THSSA^{2-} + H^+ K_2 \quad (2)$$

The acid-base equilibrium constant K_2 can be determined from the pH dependence of the ratio of TTA signal amplitudes at 440 and 470 nm ($\Delta D^{470}/\Delta D^{440}$) (Eq. (3)):

$$\frac{\Delta D^{470}}{\Delta D^{440}} = \frac{\varepsilon_2^{470}}{\varepsilon_2^{440}} \frac{(\varepsilon_1^{470}/\varepsilon_2^{470} + K_2/[H^+])}{(\varepsilon_1^{440}/\varepsilon_2^{440} + K_2/[H^+])} \quad (3)$$

where the subscripts ≪1≫ and ≪2≫ stand for $^TH_2SSA^-$ and $^THSSA^{2-}$, respectively. The absorption coefficients of $^THSSA^{2-}$ were known [20] and the ratio $\varepsilon_1^{470}/\varepsilon_1^{440} \approx 0.55$ was determined from flash photolysis experiments at pH < 2. The best fit of Eq. (3) to the experimental data (Fig. 5B) was obtained with $\varepsilon_1^{440} = (6.2 \pm 1.0) \times 10^3$ M^{-1} cm^{-1} and p$K_2 = 3.5 \pm 0.1$. The ε_1^{440} value was used to determine the T–T annihilation rate constant of $^TH_2SSA^-$ ($2k_{T-T} = (1.8 \pm 0.2) \times 10^9$ M^{-1} s^{-1}). The increase of this rate constant with decreasing pH of the medium can be explained by the decrease of the charge on the SSA dianion triplet state upon protonation.

3.2.2. *Spectrum and decay kinetics of $HSSA^{\bullet-}$ radical anion*

In oxygen-saturated solutions, both the hydrated electron and $^THSSA^{2-}$ populations decay rapidly (200 ns), allowing the absorption spectrum of the longer-lived $HSSA^{\bullet-}$ radical anion resulting from $HSSA^{2-}$ photoionization to be recorded (Fig. 6A). In neutral solution, the $HSSA^{\bullet-}$ spectrum consists of two absorption bands with maxima at 400 and 415 nm. As the pH decreases, the bands move to longer wavelength (Fig. 6A) and the decay rate constant of $HSSA^{\bullet-}$ (k_{obs}^{440}) increases (Fig. 6B).

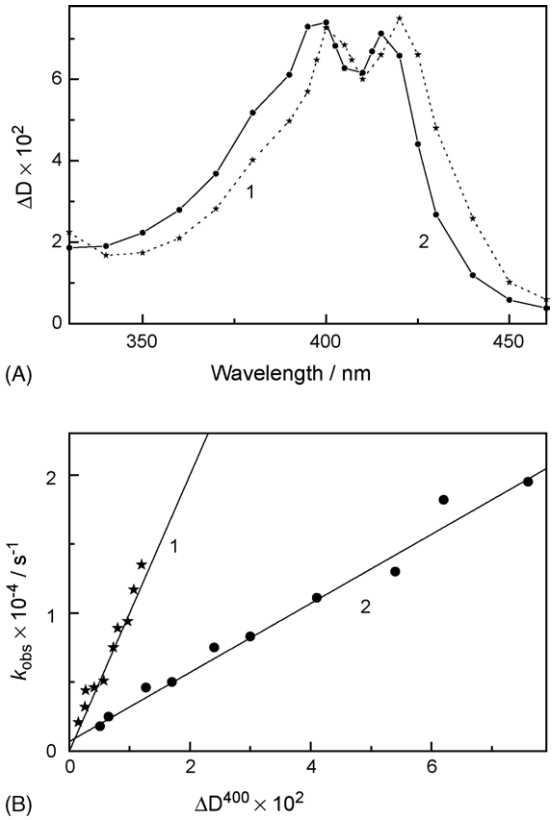

Fig. 6. (A) Transient absorption spectra obtained 1.6 μs after laser excitation of oxygen-saturated aqueous solutions of SSA (2.2×10^{-4} M) at (1) pH = 2.5 and (2) pH = 7. (B) Dependence of the observed decay rate constant k_{obs} of (1) $HSSA^{\bullet -}$ (pH = 2.5) and (2) $SSA^{\bullet 2-}$ absorption on the initial optical density at 400 nm.

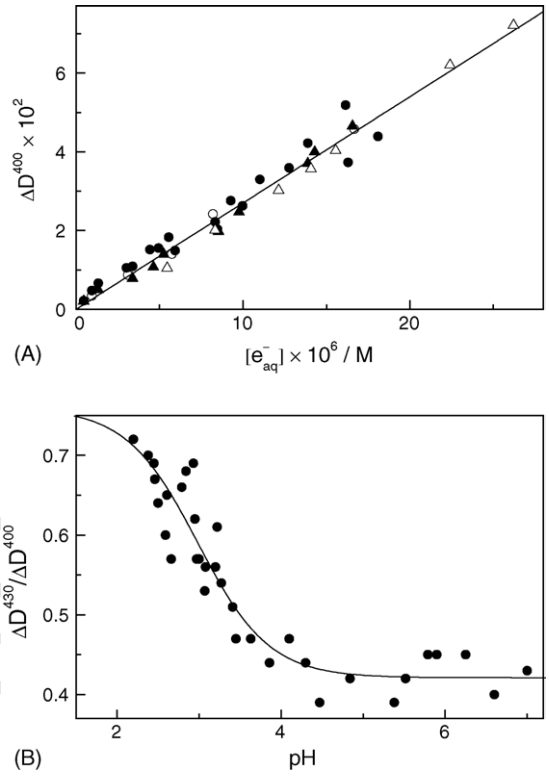

Fig. 7. (A) Dependence of ΔD^{400} on the hydrated electron concentration. Dark circles: pH = 7.0; empty circles: pH = 3.5; dark triangles: pH = 3.0; empty triangles: pH = 2.5. (B) pH dependence of the $\Delta D^{430}/\Delta D^{400}$ ratio. The solid line is the best fit of Eq. (5) with $\varepsilon_3^{430} = 2.0 \times 10^3\ M^{-1}\ cm^{-1}$ and $pK_4 = 3.1$ ([SSA] = 2.3×10^{-4} M).

Since protonation of the $HSSA^{\bullet -}$ radical anion over the pH range investigated is hardly probable (the pK_a of the phenoxyl radical is −2.0 [27]), the aforementioned results indicate a dissociation of the radical carboxyl group in the neutral medium:

$$HSSAA^{\bullet -} \Leftrightarrow SSA^{\bullet 2-}H^+ K_4 \quad (4)$$

Thus, in neutral solutions, the radical anion exists in the deprotonated form ($SSA^{\bullet 2-}$). Similarly to (Eq. (3)), the acid-base equilibrium constant K_4 can be found from:

$$\frac{\Delta D^{430}}{\Delta D^{400}} = \frac{\varepsilon_4^{430}}{\varepsilon_4^{400}} \frac{(\varepsilon_3^{430}/\varepsilon_4^{430} + K_4/[H^+])}{(\varepsilon_3^{400}/\varepsilon_4^{400} + K_4/[H^+])} \quad (5)$$

where the subscripts ≪3≫ and ≪4≫ stand for the $HSSA^{\bullet -}$ and $SSA^{\bullet 2-}$ radical anions, respectively. ε_3^{400} and ε_4^{400} were determined by measuring the magnitude of the radical anion absorption at 400 nm (ΔD^{400}) (flash photolysis of $HSSA^{2-}$ in oxygen-saturated solutions at various pH) and the concentration of hydrated electrons (flash photolysis of $HSSA^{2-}$ in oxygen-free solutions, pH = 7) at various intensities of the excitation laser pulse (Fig. 7A). Variation of the pH over a wide range (2.5–7) has almost no effect on the value of the observed absorption coefficient of radical anion at 400 nm ($\varepsilon_{obs} = (2.7 \pm 0.3) \times 10^3\ M^{-1}\ cm^{-1}$), indicating a $\varepsilon_3^{400}/\varepsilon_4^{400}$ ratio of about 1 (Fig. 7A). The $\varepsilon_4^{430}/\varepsilon_4^{400} \approx 0.42$ ratio was obtained by averaging experimental data for pH > 4 (Fig. 7B). Thus, the only unknown in Eq. (5) are ε_3^{430} and K_4. The best fit of Eq. (5) to the experimental data shown in Fig. 7B indicates a $pK_4 = 3.1 \pm 0.1$, which is close to pK_a of the carboxyl group of SSA ($pK_a = 2.9$). This confirms the hypothesis of the deprotonation of $HSSA^{\bullet -}$ radical anion in a neutral medium.

The linear dependence of k_{obs} on the absorption amplitude of $HSSA^{\bullet -}$ and $SSA^{\bullet 2-}$ at 400 nm (Fig. 6B) indicates that these radicals decay mainly upon recombination with the rate constants $2k = (2.8 \pm 0.4) \times 10^9\ M^{-1}\ s^{-1}$ and $2k = (7 \pm 0.4) \times 10^8$, respectively. The intercepts of the linear plots in Fig. 6B correspond to the reactions of $HSSA^{\bullet -}$ and $SSA^{\bullet 2-}$ with oxygen. In oxygen-saturated solutions, $[O_2] \approx 1.25 \times 10^{-3}$ M [28] and the corresponding rate constants can be estimated as $(7 \pm 3) \times 10^5\ M^{-1}\ s^{-1}$ for $HSSA^{\bullet -}$ and $(5 \pm 4) \times 10^5\ M^{-1}\ s^{-1}$ for $SSA^{\bullet 2-}$.

3.2.3. Decay kinetics of the hydrated electron

In oxygen-free neutral solutions, the population of hydrated electrons decays mainly upon reaction with $HSSA^{2-}$ dianion ($k = 2.7 \times 10^9\ M^{-1}\ s^{-1}$ [20]) and $SSA^{\bullet 2-}$ radical anion ($k = 7 \times 10^9\ M^{-1}\ s^{-1}$ [20]) and upon recombination ($2k = 1.1 \times 10^{10}\ M^{-1}\ s^{-1}$ [29]). As the pH decreases, the main decay channel of the hydrated electron is the reaction with a proton, resulting in the formation of a hydrogen atom ($H^+ + e_{aq}^- \rightarrow H^\bullet$, $k = 2 \times 10^{10}\ M^{-1}\ s^{-1}$ [29]). The hydrogen atom most probably disappears upon recombination ($2H^\bullet \rightarrow H_2$,

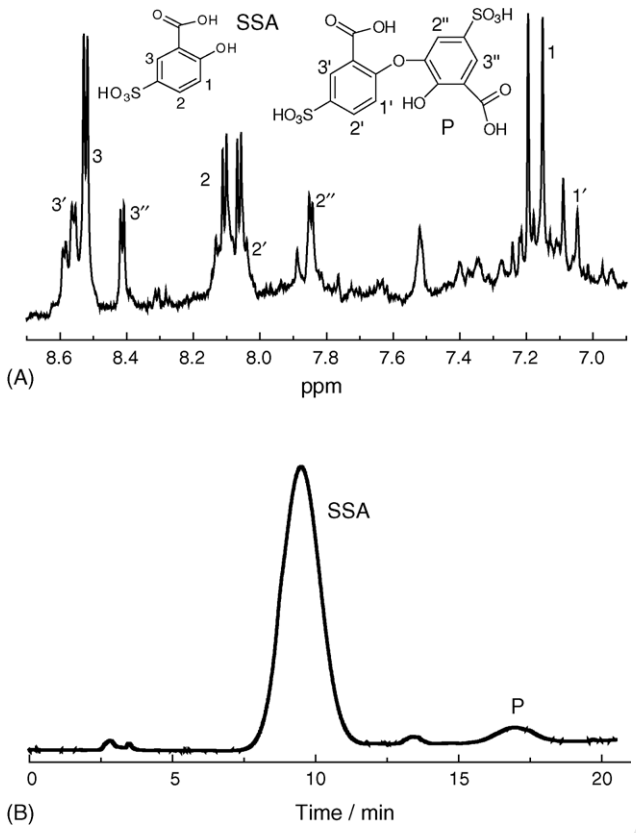

Fig. 8. (A) NMR spectrum and assignment of the product of $HSSA^{2-}$ photolysis obtained by evaporating the irradiated aqueous $HSSA^{2-}$ solution (1.3×10^{-3} M, pH = 9.5) and dissolving the dry residue in CD_3OD. (B) Chromatogram of an irradiated solution of $HSSA^{2-}$ (4.4×10^{-3} M, pH = 9.3).

$2k = 1.6 \times 10^{10}\ M^{-1}\ s^{-1}$ [29]) and in the reaction with SSA ($k = 1.4 \times 10^{9}\ M^{-1}\ s^{-1}$ for the reaction of a hydrogen atom with SA [30]).

3.3. Final products of the SSA photolysis

The NMR spectrum of an irradiated SSA dianion solution displays not only the signals of primary SSA, but also many lines corresponding to photolysis products. The strongest NMR signal belongs to the dimeric product (P), which contains five phenyl protons (Fig. 8A). The existence of only one proton signal in the high magnetic field region indicates that in the dimer, the C–O bond is the meta-position relatively to the carboxyl group. The chromatographic analysis of irradiated $HSSA^{2-}$ solutions also indicated a single main photolysis product with a retention time exceeding that of SSA (Fig. 8B). Thus, the main product of the SSA dianion photolysis is 3-(2-carboxy-4-sulfo-phenoxy)-sulfosalicylic acid resulting from the recombination of two $HSSA^{\bullet -}$ (or $SSA^{\bullet 2-}$) radicals.

4. Conclusions

The influence of the pH on the photophysical and photochemical properties of aqueous SSA solutions has been investigated. Similar to other SA derivatives SSA exhibits the large Stokes shift of fluorescence indicating the intramolecular proton transfer (or tautomerization) in the S_1 state of SSA ions. This process is responsible for the considerably lower photochemical activity of SSA monoanion compared with $HSSA^{2-}$. Excitation of $HSSA^{2-}$ gives rise to the triplet state, to the $SSA^{\bullet 2-}$ radical anion and to the hydrated electron. In neutral medium, the main decay channels of these intermediates are the T–T annihilation, the recombination and the capture by the $HSSA^{2-}$ dianion, respectively. A decrease of pH results in an increase of the second-order decay rate constants of $HSSA^{2-}$ triplet state and $SSA^{\bullet 2-}$ radical anion, because of their protonation in an acid medium. ^1H NMR was used to identify one of the final products of dianion photolysis-3-(2-carboxy-4-sulfo-phenoxy)-sulfosalicylic acid. The results indicate that the pH is an important parameter, which controls the photochemical reactions of aromatic acids in natural water.

Acknowledgements

This work was supported by the Russian Foundation for Fundamental Research (grants RFFR 05-03-32474, 03-03-33314, 03-03-39008GFEN), the Ministry of Education of RF "Universities of Russia" (grant UR.05.01.020) and the INTAS Fellowship Grant for Young Scientists 03-55-1472.

References

[1] E.M. Thurman, Organic Geochemistry of Natural Waters, Martinus Nijhoff/Dr W. Junk Publisher (Kluwer Academic Publishers Group), Dordrecht, Boston Lancaster, 1985, p. 610.
[2] Y. Zuo, J. Hoigne, Atmos. Environ. 28 (1994) 1231.
[3] W. Feng, D. Nansheng, Chemosphere 41 (2000) 1137.
[4] B.S. Faust, R.G. Zepp, Environ. Sci. Technol. 27 (1993) 2517.
[5] I.P. Pozdnyakov, E.M. Glebov, V.F. Plyusnin, V.P. Grivin, Yu.V. Ivanov, D.Yu. Vorobyev, N.M. Bazhin, Pure Appl. Chem. 72 (2000) 2187–2197.
[6] I.P. Pozdnyakov, Yu.A. Sosedova, V.F. Plyusnin, V.P. Grivin, E.M. Glebov, D.Yu. Vorobyev, N.M. Bazhin, Int. J. Photoenergy 6 (2004) 89–93.
[7] B. Voelker, F.M.M. Morel, B. Sulzberger, Environ. Sci. Technol. 31 (1997) 1004–1011.
[8] H. Gao, R.G. Zepp, Environ. Sci. Technol. 32 (1998) 2940–2946.
[9] C.J. Miles, P.L. Brezonik, Environ. Sci. Technol. 15 (1981) 1089–1095.
[10] F.J. Stevenson, Humus Chemistry, 2nd ed., John Willey & Sons, New York, 1994.
[11] P.B. Bisht, M. Okamoto, S. Hirayama, J. Phys. Chem. B 101 (1997) 8850–8855.
[12] H.-C. Ludemann, F. Hillenkamp, R.W. Redmond, J. Phys. Chem. A 104 (2000) 3884–3893.
[13] J.L. Herek, S. Pedersen, L. Banares, A.H. Zewail, J. Chem. Phys. 97 (1992) 9046–9061.
[14] C. Chen, S.-F. Shyu, J. Mol. Struct. (Theochem.) 536 (2001) 25–39.
[15] L.A. Helmbrook, J.E. Kenny, B.E. Kohler, G.W. Scott, J. Phys. Chem. 87 (1983) 280–289.
[16] L. Kozma, I. Khornyak, I. Eroshtyak, B. Nemet, J. Appl. Spec. 53 (1990) 259–265, Russian.
[17] G.S. Denisov, N.S. Golubev, V.M. Schreiber, Sh.S. Shajakhmedov, A.V. Shurukhina, J. Mol. Struct. 436–437 (1997) 153–160.
[18] P.J. Kovi, C.L. Miller, S.G. Schulman, Anal. Chim. Acta 61 (1972) 7–13.
[19] H.C. Joshi, H. Mishra, H.B. Tripathi, J. Photochem. Photobiol. A: Chem. 105 (1997) 15–20.
[20] I.P. Pozdnyakov, V.F. Plyusnin, V.P. Grivin, D.Yu. Vorobyev, A.I. Kruppa, H. Lemmetyinen, J. Photochem. Photobiol. A: Chem. 162 (2004) 153–162.
[21] D.F. Eaton, Pure Appl. Chem. 60 (1988) 1107–1114.

[22] R.H. Compton, T.U. Gratton, T. Morrow, J. Photochem. 14 (1980) 61.
[23] L. Lang, Absorption Spectra in the Ultraviolet and Visible Region, vol. 1, Academiai Kiado, Budapest, 1966, p. 93.
[24] A.K. Babko, A.T. Pilipenko, Photometric Analysis. General Information and Apparatus, Khimiya, Moscow, 1968, p. 387 (Russian).
[25] P.B. Bisht, H. Petek, K. Yoshihara, U. Nagashima, J. Chem. Phys. 103 (1995) 5290.
[26] A.K. Pikaev, S.A. Kabakchi, I.E. Makarov, B.G. Ershov, Pulse Radiolysis and its Application, Atomizdat, Moscow, 1980, p. 280 (Russian).
[27] W.T. Dixon, D. Murphy, J. Chem. Soc. Faraday Trans. II 7 (1976) 1221.
[28] V.E. Kogan, V.M. Fridman, V.V. Kafarov, Handbook of Solubility, vol. 1.N.1, USSR Academy of Sciences, Moscow, 1962, p. 87 (Russian).
[29] G.V. Buxton, C.L. Greenstock, W.P. Helman, A.B. Ross, J. Phys. Chem. Ref. Data 17 (1988) 513–886.
[30] C.B. Amphlett, C.E. Adams, B.D. Michael, Adv. Chem. Ser. 81 (1968) 231–250.